Stabilization of multiarmed spiral waves by circularly polarized electric fields

Ling-Yun Deng, Hong Zhang,* and You-Quan Li

Zhejiang Institute of Modern Physics and Department of Physics, Zhejiang University, Hangzhou 310027, China

The influence of circularly polarized electric fields (CPEFs) on the stability of multiarmed spiral waves is investigated. It is shown that CPEFs can change the period of the multiarmed spirals. The average period is an important quantity of multiarmed spiral and it must be larger than a threshold for stable multiarmed spiral. After a counter-rotating CPEF with suitable amplitude and period is applied, the average period of the multi-armed spiral may increase, which stabilizes the multiarmed spiral.

PACS number(s): 82.40.Ck, 05.65.+b, 05.45.−a

I. INTRODUCTION

Excitable media derive much of their interest from varied and sometimes unexpected spatiotemporal wave patterns owing to their nonlinearity. All excitable systems share certain characteristic features. They have a stable rest state, and small perturbations from the rest state are rapidly damped out. However, disturbances that cross a certain threshold trigger an abrupt and substantial response. Spiral waves have been observed in a variety of excitable systems such as the Belousov-Zhabotinsky (BZ) reaction [1], the cardiac tissue [2,3], and the catalytic surface processes [4]. Two or more same-chirality spirals can form multiarmed spirals (bound states of same-chirality spirals) whose tips are separated by less than a core diameter. A series of studies, both experimental and theoretical, reports multiarmed spirals [5–17]. They have been observed in BZ reaction [5], Dictyostelium discoideum [8], the whole rabbit heart [9], two-dimensional cultured heart tissue [10], etc. Zaritski *et al.* in [15] studied multiarmed spirals in a variety of numerical reaction-diffusion models of excitable media. In Ref. [17], the dynamics of multiarmed spirals in a generic reaction-diffusion model of an excitable medium is described in detail.

Since the spirals in cardiac muscle play an essential role in heart diseases such as arrhythmia and fibrillation [3,18–21], the leading cause of death in the industrialized world, the control of spirals is of crucial importance. Additionally, all realistic media are embedded in some environment and thus undergo external forces and fields. In order to understand or control the dynamics of a spiral, many experiments have been performed (usually in BZ systems). The common methods to do this are using light to illuminate a photosensitive variant of the BZ reaction [22], which leads to a change in the excitability of the system, or applying an electric field, [23] which introduces a drift of ionic key species of the reaction. However, all these works considered only one-armed spirals while the influence of external forces and fields on multiarmed spirals has not been investigated yet.

In a previous paper, we investigated the drift behavior of one-armed spirals induced by a polarized electric field in a reaction-diffusion model in the light that both the spiral and the circularly polarized electric field (CPEF) possess the rotation symmetry [24]. It is worthwhile for us to study the influence of CPEFs on multiarmed spirals that also possess the rotation symmetry in present paper.

II. MODEL

We consider the effect of an electric field on spiral dynamics using a two-variable reaction-diffusion model with an additional gradient term $\mathbf{E} \cdot \nabla u$ [25],

$$\frac{\partial u}{\partial t} = \frac{1}{\varepsilon} f(u,v) + \nabla^2 u + \mathbf{E} \cdot \nabla u, \tag{1a}$$

$$\frac{\partial v}{\partial t} = g(u,v). \tag{1b}$$

The variables u and v can be viewed as the "fast" and "slow" variables; ε is a parameter characterizing the excitability of the medium and $\varepsilon=0.02$ is used for all results reported in this paper; and $\mathbf{E}=(E_x,E_y)$ is the electric field and the additional term $\mathbf{E} \cdot \nabla u = E_x \partial u / \partial x + E_y \partial u / \partial y$. A CPEF is composed of two ac electric fields, $E_x=E_0 \cos(\omega t)$ and $E_y=E_0 \cos(\omega t + \phi)$, which are applied along the x and y axes, respectively, and their superposition $\mathbf{E}$ rotates with angular frequency ω in two-dimensional space [24]. A CPEF rotates clockwise for the phase difference $\phi=\pi/2$, while it rotates anticlockwise for $\phi=3\pi/2$. For numerical simulations, we will consider a modified FitzHugh-Nagumo model [26], where $f(u,v)=u(1-u)[u-(v+b)/a]$ and $g(u,v)=u-v$. The advantage of this model is that it permits fast calculations and catches the essential features of excitable media. Numerical simulations are carried out on 320×320 or 600×600 grid points employing the explicit Euler method. The space and time step are $\Delta x=\Delta y=0.1826$ and $\Delta t=0.005$, respectively. No-flux conditions are imposed at the boundaries.

In Ref. [17], Zemlin *et al.* explored the phase diagram of multiarmed spiral in the plane of parameters $a-b$; the multiarmed spiral state exists only in a stripelike region. Generally, the spiral solution with rigid rotation of a reaction-diffusion model takes the form [5]

$$u = u(N\theta - \omega t + \alpha, r), \quad v = v(N\theta - \omega t + \beta, r),$$

where ω is the angular velocity, α and β are two phase shifts,

*Author to whom correspondence should be addressed; hongzhang@zju.edu.cn and hzhang@zimp.zju.edu.cn
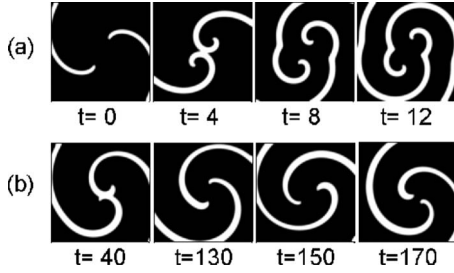
036107-1

FIG. 1. Typical snapshots during the evolution of system (1) at $a=1.1$ and $b=0.2$ (a) without external fields (b) in the presence of a counter-rotating CPEF with $E_0=1.0$ and $\omega=\omega_0=1.22$, where ω_0 is the average frequency of the single-armed spiral with the same parameters. The simulation is performed on a square grid containing 320×320 grid points. To create the initial condition ($t=0$), we superimpose snapshots of a single-armed spiral in equally spaced phases, i.e., sum the values of each variable over the different snapshots at each point of the medium.

and the topological charge N characterizes the number of arms and the direction of the rotation ($N=\pm1$, a one-armed spiral rotating clockwise or anticlockwise; $N=\pm2$, a two-armed spiral).

III. RESULTS AND DISCUSSION

An initial two-armed spiral [Fig. 1(a), $t=0$] is created by superimposing snapshots of a single-armed spiral in equally spaced phases. At parameters $a=1.1$ and $b=0.2$, there is no stable multiarmed spiral [17] and this initial two-armed spiral is not stable and will decay into two single-armed spirals, as shown in Fig. 1(a). However, when a suitable CPEF is introduced, the phenomenon is dramatically changed. In Fig. 1(b), a counter-rotating CPEF with $E_0=1.0$ and $\omega=\omega_0$ is applied to the initial two-armed spiral and one can see that the two-armed spiral is stabilized finally. Comparing Fig. 1(a) with Fig. 1(b), one can see that the CPEF makes a strong impact on the stability of multiarmed spirals. To our knowledge, only the impact of localized defect on multiarmed spirals is studied [6,7] and little is known about the influence of external forces and fields on multiarmed spirals. Differing from localized defect, CPEFs are spatially homogeneous and can be realized by adding two ac electric fields perpendicular to each other.

In Fig. 2(a), the corresponding tip trajectories of the stabilized two-armed spiral are shown. When the two tips are far from each other, their interaction is weak and they meander in their own way. When they move toward each other, their interaction is strong and at a critical distance they will collide. After the collision, the directions of motion of the two tips are changed evidently and they meander in their own way again. Figure 2(b) shows the distance between the tips as a function of time; it varies periodically. The minimal distance corresponds to the collision in Fig. 2(a).

It is then interesting to understand the mechanism underlying the above results. As the excitability of weakly excitable medium increases the one-armed spiral core radius decreases and the front interface begins to feel the medium disturbance due to the spiral previous passages; this eventu-
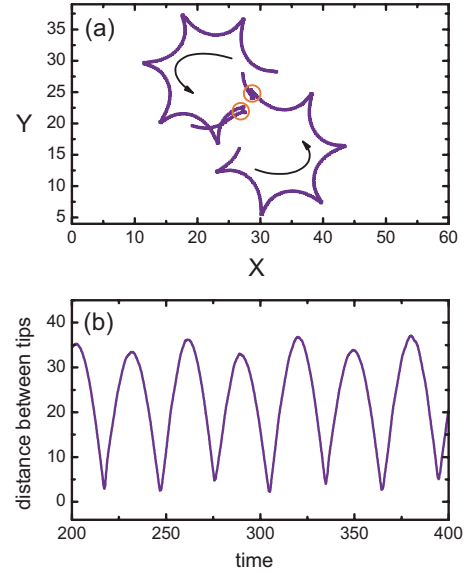

FIG. 2. (Color online) (a) Tip trajectories of a stabilized two-armed spiral under the control of a counter-rotating CPEF. When getting close to each other, the two tips collide (marked by two circles). After that, the tips dramatically change their directions of motion and then they meander in their own way. (b) The distance between the two tips as a function of time. The minima occur when the tips collide. Numerical simulations are carried out in a box with 320×320 grid points and the parameters are $a=1.1$, $b=0.2$, $E_0=1.4$, and $\omega=\omega_0=1.22$.

ally leads to spiral meander due to the self-interaction of the wave front with its own recovery tail [27]. While for the two-armed spiral, one arm will interact with the exponential recovery tail of the controller field v of the other arm instead of its own recovery tail. Thus the average period or the average frequency may be an important quantity characterizing the multiarmed spiral waves [6,13] since the two arms will interact with each other strongly (repel each other) and the two-armed spiral will not be stable when the average frequency is high (or the average period is short). In Ref. [8], Vasiev *et al.* showed that for the fixed refractoriness of the medium, the maximum number of arms of multiarmed spiral increases with an increase in the rotation period of a single-armed spiral.

To give an understanding of the stabilization of two-armed spiral waves by CPEFs, let us investigate one-armed spirals first. In Fig. 3, we give the average period, the average wavelength, and the average wave speed of the one-armed spiral as a function of the parameter b with $a=1.1$. For the one-armed spiral without control, the average period and the average wavelength decrease as we diminish b [squares in Figs. 3(a) and 3(b)]. When we add a counter-rotating CPEF with $E_0=0.5$ and $\omega=\omega_0$ to the system, the average period and the average wavelength increase [circles in Figs. 3(a) and 3(b)], while for the average wave speed, it changes little after we apply the CPEF [Fig. 3(c)]. From the results of one-armed spirals, one can make a conjecture that the average periods and the average wavelength of the two-armed spirals will increase after a suitable counter-rotating CPEF is applied.

The average period of a two-armed spiral as a function of b is given in Fig. 4(a). The average period of the free two-
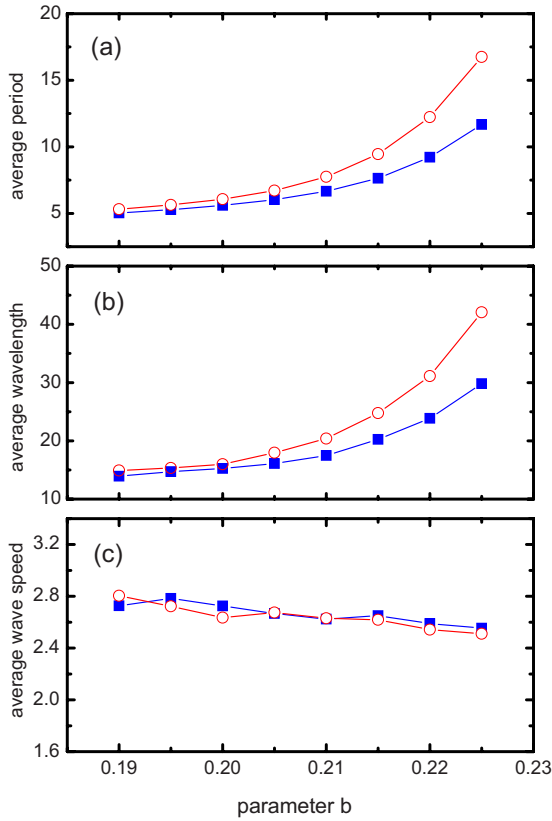
FIG. 3. (Color online) The dependences of (a) the average period, (b) the average wavelength, and (c) the average wave speed of the single-armed spiral on the parameter b for $a=1.1$. Grid 600×600 points. Squares: without control; circles: under the control of a counter-rotating CPEF with $E_0=0.5$ and $\omega=\omega_0$ (ω_0 takes different values for different b). The average period is sensed by a probe far from spiral tip, and it is averaged over time. The average wavelength is the distance between two adjacent maxima of variable u along radial direction in the region far from spiral tip, and it is averaged over different directions. The average wave speed equals the average wavelength divided by the average period. The driving period ($2\pi/\omega$) equals the average period of the spiral without control ($2\pi/\omega_0$), i.e., the squares in (a).
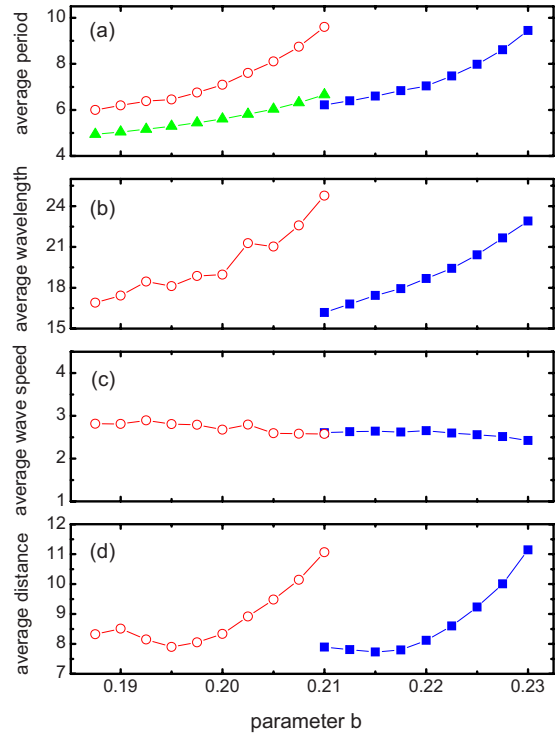

FIG. 4. (Color online) The dependences of (a) the average period, (b) the average wavelength, (c) the average wave speed, and (d) the average distance between tips of the two-armed spiral on the parameter b. Squares: without control; circles: under the control of a counter-rotating CPEF with $E_0=0.5$ and $\omega=\omega_0$, where ω_0 is the average period of single-armed spiral without control; and triangles: the driving period $2\pi/\omega$. The other parameters are the same as in Fig. 3.

armed spiral decreases as we diminish b. Once the average period is lower than a threshold—6.2, where $b=0.21$—the two-armed spiral would not be stable anymore, and it will decay into two single-armed spirals. However, when we add a counter-rotating CPEF with $E_0=1.0$ and $\omega=\omega_0$ to the system, the average period is increased remarkably [circles in Fig. 4(a)]. The interaction between these two arms now becomes weak, i.e., the repulsion is not strong enough to separate the two spiral tips; this actually stabilizes the two-armed spiral. We conclude that it is the increasing of the average period of the two-armed spiral by CPEFs that stabilizes the two-armed spiral. Then, the parameter region that supports stable two-armed spiral is extended by the external electric field [from $b=0.21$ to $b=0.1875$, see Fig. 4(a) for detail]. The threshold of the average period is now 6.0 which is almost the same as the case without control. From above results, one can see that the average period is an important

quantity that may characterize the stability of two-armed spirals. In Fig. 4(b), we give the dependence of the average wavelength on b which is similar to the case of the average period. Figure 4(c) shows that the average wave speed of the two-armed spiral almost keeps invariant when the CPEF is applied. In Fig. 4(d), we also give the dependence of the average distance between the two tips on b. Different from the average period, the average distance does not monotonously decrease as we diminish b. Instead, the average distance has a local minimal value at $b=0.215$ in the case of the spiral being free and at $b=0.195$ in the case of the spiral being controlled by the counter-rotating CPEF.

In order to give a complete description about the spiral patterns controlled by circularly polarized electric fields, we present distributions of patterns in the E_0-ω plane in Fig. 5. Three types of phenomena are observed: (1) the two-armed spiral is not stabilized and it decays into two single-armed spirals (region "SS" in Fig. 5); (2) the two-armed spiral is stabilized (region "TS" in Fig. 5) ; and (3) the two-armed spiral waves break up (region "BU" in Fig. 5). The stability of a two-armed spiral was assumed if it showed no sign of decay after 100 spiral rotations. In the TS regime, for fixed ω, the wavelength of the stabilized two-armed spiral increases with E_0, i.e., the two-armed spiral waves become sparse as we strengthen the electric field; for fixed E_0, the average period of the stabilized two-armed spiral decreases
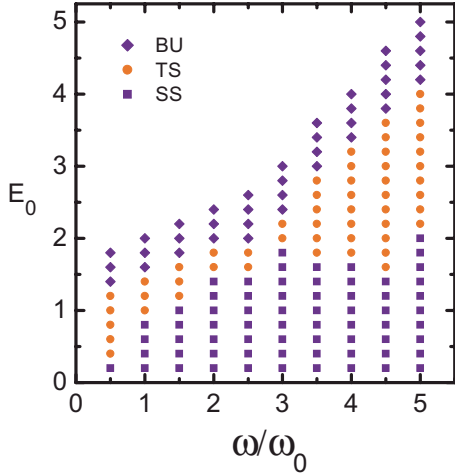
FIG. 5. (Color online) The pattern phase diagram in the E_0-ω plane for $a=1.1$, $b=0.19$, and $\omega_0=1.24$. Grid 600×600 points. Region "TS" means that the two-armed spiral is stable. Below the region TS, the electric field is not strong enough to stabilize the two-armed spiral and it decays into two single-armed spirals (region "SS"), and above the region TS, the electric field is so strong that the two-armed spiral may break up (region "BU"). The initial pattern is a two-armed spiral created by superimposing snapshots of a single-armed spiral in equally spaced phases.

when we increase ω. Below the TS regime, i.e., the SS regime, the electric filed is not strong enough to stabilize the two-armed spiral, and therefore only single-armed spirals exist. In the BU regime which is above the TS regime, the electric filed is so strong that the spiral waves break up. After they break up, the system will evolve into one of following three states (the details are not shown in Fig. 5): spiral pattern (including single-armed spiral or two-armed spiral), rest state, or complicated pattern.

In all above discussions, only counter-rotating circularly polarized electric fields are investigated. It is also interesting to study what happens when two-armed spirals are forced with elliptically, linearly, or corotating circularly polarized electric fields. Here, we do some numerical simulations to test the effects of a polarized electric field composed of two ac electric fields $E_x=E_0\cos(\omega t)$ and $E_y=E_0\cos(\omega t+\phi)$, where $\phi=0,\pi/4,\pi/2,3\pi/4,\pi,5\pi/4,3\pi/2,7\pi/4$. When
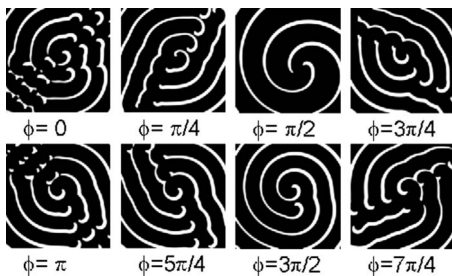

FIG. 6. The final patterns controlled by CPEFs with different phase differences from an initial two-armed spiral. The parameters here are $E_0=1.0$, $\omega=\omega_0=0.943$, $a=1.1$, and $b=0.21$. Grid 600×600 points.
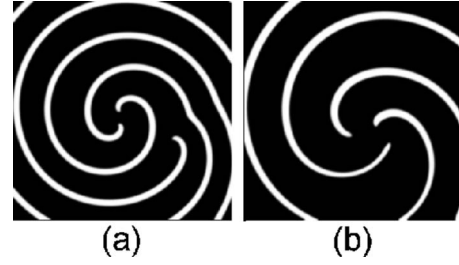

FIG. 7. States evolved from an initial three-armed spiral that is created by superimposing snapshots of a single-armed spiral in equally spaced phases (a) without external fields (b) in the presence of a counter-rotating CPEF with $E_0=0.7$ and $\omega=0.5\omega_0$ (ω_0 $=0.732$). The other parameters are $a=1.2$ and $b=0.25$. Grid 600×600 points.

$\phi=0,\pi$ the electric field is linearly polarized, when $\phi=3\pi/2$ it is circularly polarized and its rotation direction is the same as that of the studied spiral, when $\phi=\pi/2$ it is circularly polarized and it rotates in the opposite direction to the studied spiral, and when $\phi=\pi/4,3\pi/4,5\pi/4,7\pi/4$ it is elliptically polarized [24]. Under the control of these electric fields, the two-armed spiral may change to three types of final patterns (cf. Fig. 6): breaking waves when $\phi=0,\pi/4,3\pi/4,\pi,5\pi/4,7\pi/4$ (linearly or elliptically polarized electric field); two single-armed spirals when $\phi=3\pi/2$ (corotating CPEF); and stabilized two-armed spiral when $\phi=\pi/2$ (counter-rotating CPEF). The results show that only counter-rotating CPEFs can stabilize two-armed spirals. Although a corotating CPEF does not make the spiral waves break up, it can destabilize the two-armed spiral. For example, a corotating CPEF with $E_0=0.15$ and $\omega=\omega_0$ shrinks the range that supports two-armed spirals in Fig. 4(a) from $b\geq0.21$ to $b\geq0.23$.

Aside from two-armed spirals, three-armed spirals can also be stabilized by CPEFs in the parameter region where it was unstable. Figure 7(a) is one state evolved from an initial three-armed spiral without control. One can see that the initial three-armed spiral is not stable and it decays into one two-armed spiral and one single-armed spiral. Figure 7(b) is the final state evolved from the initial three-armed spiral controlled by a counter-rotating CPEF with $E_0=0.7$ and $\omega=0.5\omega_0$. After a transient time, the initial three-armed spiral is stabilized.

IV. CONCLUSIONS

We have studied the influence of CPEFs on multiarmed spiral waves. It is shown that the period of the two-armed spiral plays an important role in determining whether the multiarmed spiral is stable or not. When the average period is lower than a threshold magnitude, the repulsion between two arms becomes so strong that the two-armed spiral will decay into two single-armed spirals. We find that a counter-rotating CPEF with suitable amplitude and period can increase the period of the two-armed spiral. This weakens their

interaction, which may stabilize the two-armed spiral. Moreover, we have shown that three-armed spirals can also be stabilized by CPEFs in the parameter region where it was unstable. At last, we expect that our results can be observed in experiments.

[1] A. T. Winfree, Science **175**, 634 (1972).

[2] M. A. Allessie, F. I. M. Bonke, and F. J. G. Schopman, Circ. Res. **33**, 54 (1973).

[3] J. M. Davidenko, A. V. Pertsov, R. Salomonsz, W. Baxter, and J. Jalife, Nature (London) **355**, 349 (1992).

[4] S. Jakubith, H. H. Rotermund, W. Engel, A. von Oertzen, and G. Ertl, Phys. Rev. Lett. **65**, 3013 (1990).

[5] K. I. Agladze and V. I. Krinsky, Nature (London) **296**, 424 (1982).

[6] O. Steinbock and S. C. Müller, Int. J. Bifurcation Chaos Appl. Sci. Eng. **3**, 437 (1993).

[7] S. Nettesheim, A. von Oertzen, H. H. Rotermund, and G. Ertl, J. Chem. Phys. **98**, 9977 (1993).

[8] B. Vasiev, F. Siegert, and C. Weijer, Phys. Rev. Lett. **78**, 2489 (1997).

[9] T. J. Wu, M. A. Bray, C. T. Ting, and S. F. Lin, J. Cardiovasc. Electrophysiol. **13**, 414 (2002).

[10] N. Bursac, F. Aguel, and L. Tung, Proc. Natl. Acad. Sci. U.S.A. **101**, 15530 (2004).

[11] S. M. Hwang, T. Y. Kim, and K. J. Lee, Proc. Natl. Acad. Sci. U.S.A. **102**, 10363 (2005).

[12] L. Dong, H. Wang, F. Liu, and Y. He, New J. Phys. **9**, 330 (2007).

[13] E. A. Ermakova, A. M. Pertsov, and E. E. Shnol, Physica D **40**, 185 (1989).

[14] R. M. Zaritski and A. M. Pertsov, Phys. Rev. E **66**, 066120 (2002).

[15] R. M. Zaritski, J. Ju, and I. Ashkenazi, Int. J. Bifurcation Chaos Appl. Sci. Eng. **15**, 4087 (2005).

[16] C. Zemlin, K. Mukund, M. Wellner, R. Zaritsky, and A. Pertsov, Phys. Rev. Lett. **95**, 098302 (2005).

[17] C. W. Zemlin, K. Mukund, V. N. Biktashev, and A. M. Pertsov, Phys. Rev. E **74**, 016207 (2006).

[18] R. A. Gray, A. M. Pertsov, and J. Jalife, Nature (London) **392**, 75 (1998).

[19] F. X. Witkowski, L. J. Leon, P. A. Penkoske, W. R. Giles, M. L. Spano, W. L. Ditto, and A. T. Winfree, Nature (London) **392**, 78 (1998).

[20] S. Alonso, F. Sagués, and A. S. Mikhailov, Science **299**, 1722 (2003).

[21] H. Zhang, Z. Cao, N. J. Wu, H. P. Ying, and G. Hu, Phys. Rev. Lett. **94**, 188301 (2005); Z. Cao, P. Li, H. Zhang, F. Xie, and G. Hu, Chaos **17**, 015107 (2007).

[22] K. I. Agladze, V. A. Davydov, and A. S. Mikhailov, JETP Lett. **45**, 767 (1987); A. Schrader, M. Braune, and H. Engel, Phys. Rev. E **52**, 98 (1995); V. S. Zykov, O. Steinbock, and S. C. Müller, Chaos **4**, 509 (1994); R. M. Mantel and D. Barkley, Phys. Rev. E **54**, 4791 (1996); I. V. Biktasheva and V. N. Biktashev, *ibid.* **67**, 026221 (2003); H. Zhang, N. J. Wu, H. P. Ying, G. Hu, and B. Hu, J. Chem. Phys. **121**, 7276 (2004).

[23] O. Steinbock, J. Schütze, and S. C. Müller, Phys. Rev. Lett. **68**, 248 (1992); K. I. Agladze and P. De Kepper, J. Phys. Chem. **96**, 5239 (1992); V. Krinsky, E. Hamm, and V. Voignier, Phys. Rev. Lett. **76**, 3854 (1996); A. P. Muñuzuri, M. Gómez-Gesteira, V. Pérez-Muñuzuri, V. I. Krinsky, and V. Pérez-Villar, Phys. Rev. E **48**, R3232 (1993); M. Wellner, A. M. Pertsov, and J. Jalife, *ibid.* **59**, 5192 (1999); H. Zhang, B. Hu, G. Hu, and J. Xiao, J. Chem. Phys. **119**, 4468 (2003); H. Henry, Phys. Rev. E **70**, 026204 (2004); H. Zhang, J. X. Chen, L. Q. Li, and J. Xu, J. Chem. Phys. **125**, 204503 (2006).

[24] J. X. Chen, H. Zhang, and Y. Q. Li, J. Chem. Phys. **124**, 014505 (2006).

[25] For examples, see J. Schütze, O. Steinbock, and S. C. Müller, Nature (London) **356**, 45 (1992); J. J. Taboada, A. P. Muñuzuri, V. Pérez-Muñuzuri, M. Gómez-Gesteira, and V. Pérez-Villar, Chaos **4**, 519 (1994); B. Schmidt and S. C. Müller, Phys. Rev. E **55**, 4390 (1997).

[26] D. Barkley, M. Kness, and L. S. Tuckerman, Phys. Rev. A **42**, R2489 (1990).

[27] V. Hakim and A. Karma, Phys. Rev. E **60**, 5073 (1999).